Proceedings of the 2008 IEEE
International Conference on Robotics and Biomimetics
Bangkok, Thailand, February 21 - 26, 2009

Reactionless Resolved Acceleration Control with Vibration Suppression Capability for JEMRMS/SFA

Yusuke Fukazu[1], Naoyuki Hara[1], Yoshikazu Kanamiya[2] and Daisuke Sato[2]
Depertment of Mechanical Systems Engineering
Musashi Institute of Technology (Tokyo City University, after April 2009)
1-28-1 Tamazutsumi, Setagaya-ku, Tokyo 158-8557, Japan
[1]{*fukazu,hara*}*@rls.mes.musashi-tech.ac.jp,* [2]{*nenchev,sato*}*@ieee.org*

***Abstract*—We propose an integrated motion controller for the Japanese Experimental Module RMS/SFA "macro-mini" manipulator system on the International Space Station. This controller is based on the Reaction Null-Space concept described in previous works. The performance of this controller with a planar flexible-base manipulator has been studied in [1]. Here, we show how to implement the controller for the JEMRMS/SFA system and examine its performance via simulations. Results show that end-effector path tracking combined with reactionless motion and vibration suppression can be achieved in a stable way, by making use of the inherent kinematic/dynamic redundancies of the system.**

***Index Terms*—Macro-mini manipulator, space robot, redundant flexible-base manipulator, vibration suppression control, reaction null space control.**

I. Introduction

Flexible-base manipulators have been studied widely in the past, in view of two main fields of application: nuclear waste cleanup [2], [3] and space robotics [4], [5]. In the former application, a manipulator is mounted on a long beam to ensure access to a remote site. In the latter application, the manipulator is mounted at the end of a large arm that can relocate the manipulator base to a desired position. Examples include the Canadian SSRMS/Dextre [6] and the JEMRMS/SFA[1] (Fig. 1) manipulator systems on the International Space Station. We will refer to such systems as "macro-mini manipulator systems." Once the manipulator is relocated, it will start accomplishing various dexterous tasks. During these operations, the joints of the large arm are usually locked, and thus, the arm can be regarded as a flexible-base for the manipulator. Another representative class of flexible-base manipulators are lightweight humanoid robots that may vibrate in response to reactions from arm motions [7].

Flexible-base manipulators induce base vibrations via the reaction force. A few control methods have been proposed in the past that can ensure base vibration suppression control [8]–[11], design of control inputs that induce minimum vibrations [12], end-point control in the presence of vibrations [13], [14], and optimal control [15]. Appropriate control methods depend very much on the structure of the manipulator, e.g. dual-arm or single-arm, and the presence of kinematic and/or dynamic redundancy.

[1]Japanese Experimental Module Remote Manipulator System/Small Fine Arm.

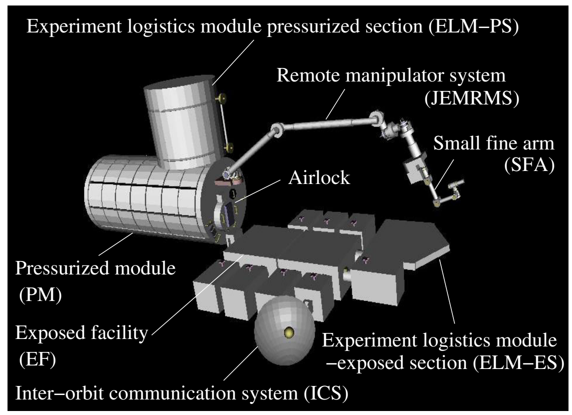

Fig. 1. Japanese experimental module "Kibo" with attached JEMRMS/SFA.

In this work, we focus on a kinematically/dynamically redundant flexible base manipulator. End-effector control in the presence of base vibrations becomes possible with such a manipulator. In addition, there is also a possibility for vibration suppression control via manipulator self-motion. In fact, only a few works have considered so far simultaneous end-effector motion and vibration suppression control [16], [17], [18].

The main aim of this work is to propose a model and a control law for a real macro-mini manipulator system — the JEMRMS with attached SFA. We will show that the Reaction Null-Space based control law, as proposed originally in [1], is useful to achieve the task of simultaneous end-effector motion and vibration suppression control.

II. Background and Notation

A. Equation of Motion

The equation of motion of an n-DOF manipulator, mounted on a flexible base with k flexural coordinates, has the form of an underactuated system. It can be written as follows [19]:

$$\begin{bmatrix} \boldsymbol{H}_b & \boldsymbol{H}_{bm} \\ \boldsymbol{H}_{bm}^T & \boldsymbol{H}_m \end{bmatrix} \begin{bmatrix} \dot{\boldsymbol{\nu}}_b \\ \ddot{\boldsymbol{q}} \end{bmatrix} + \begin{bmatrix} \boldsymbol{D}_b & \boldsymbol{0} \\ \boldsymbol{0} & \boldsymbol{D}_m \end{bmatrix} \begin{bmatrix} \boldsymbol{\nu}_b \\ \boldsymbol{q} \end{bmatrix} + \begin{bmatrix} \boldsymbol{K}_b & \boldsymbol{0} \\ \boldsymbol{0} & \boldsymbol{0} \end{bmatrix} \begin{bmatrix} \Delta\boldsymbol{\xi}_b \\ \boldsymbol{q} \end{bmatrix} + \begin{bmatrix} \boldsymbol{c}_b \\ \boldsymbol{c}_m \end{bmatrix} = \begin{bmatrix} \boldsymbol{0} \\ \boldsymbol{\tau} \end{bmatrix}, \quad (1)$$

where $\Delta\boldsymbol{\xi}_b \in \Re^k$ is the positional/orientational deflection of the flexible base from its equilibrium, $\boldsymbol{\nu}_b \in \Re^k$ is the base twist (spatial velocity), $\boldsymbol{q} \in \Re^n$ stands for the joint coordinates of the arm, $\boldsymbol{H}_b(\Delta\boldsymbol{\xi}_b, \boldsymbol{q})$, $\boldsymbol{D}_b$ and $\boldsymbol{K}_b \in \Re^{k\times k}$ denote base inertia, damping and stiffness, respectively. $\boldsymbol{H}_m(\boldsymbol{q}) \in \Re^{n\times n}$ is the inertia matrix of the arm. $\boldsymbol{H}_{bm}(\Delta\boldsymbol{\xi}_b, \boldsymbol{q}) \in \Re^{k\times n}$ denotes the *inertia coupling matrix*. $\boldsymbol{c}_b(\Delta\boldsymbol{\xi}_b, \boldsymbol{\nu}_b, \boldsymbol{q}, \dot{\boldsymbol{q}})$ and $\boldsymbol{c}_m(\Delta\boldsymbol{\xi}_b, \boldsymbol{\nu}_b, \boldsymbol{q}, \dot{\boldsymbol{q}})$ are velocity-dependent nonlinear terms. $\boldsymbol{D}_m$ denotes joint damping and $\boldsymbol{\tau} \in \Re^n$ is the joint torque.

Below we will consider two independent control approaches.

B. Vibration Suppression Control

The upper part of the equation of motion (1) can be linearized around the equilibrium of the base:

$$\boldsymbol{H}_b\dot{\boldsymbol{\nu}}_b + \boldsymbol{D}_b\boldsymbol{\nu}_b + \boldsymbol{K}_b\Delta\boldsymbol{\xi} = -\boldsymbol{H}_{bm}\ddot{\boldsymbol{q}}. \tag{2}$$

Note that the nonlinear term $\boldsymbol{c}_b$ has been assumed to be sufficiently small and its contribution is ignored. Then, we can choose the control acceleration as

$$\ddot{\boldsymbol{q}}_{vs} = \boldsymbol{H}_{bm}^{+}\boldsymbol{G}_b\boldsymbol{\nu}_b. \tag{3}$$

Here, $\boldsymbol{G}_b$ denotes a constant positive definite damping matrix, and $(\circ)^+$ stands for the pseudoinverse. It should be then apparent that controlled damping can be achieved via inertial coupling.

C. Reactionless Motion Control

The wrench, imposed on the base in the form of reaction from manipulator motion, can be rewritten as follows:

$$\boldsymbol{w}_b = \boldsymbol{H}_{bm}\ddot{\boldsymbol{q}} + \dot{\boldsymbol{H}}_{bm}\dot{\boldsymbol{q}}. \tag{4}$$

The integral of the dynamics (4), denoted as

$$\boldsymbol{L} = \boldsymbol{H}_{bm}\dot{\boldsymbol{q}} + \boldsymbol{C} \tag{5}$$

is called *the coupling momentum* [1]. The manipulator does not induce any reactions to the base, if the coupling momentum is conserved: $\boldsymbol{L} = \mathbf{const} \Leftrightarrow \boldsymbol{w}_b = \boldsymbol{0}$. The proof follows from the direct examination of (4) and (5).

Zero reaction/coupling momentum conservation is achieved with the joint acceleration:

$$\ddot{\boldsymbol{q}}_{rm} = -\boldsymbol{H}_{bm}^{+}\dot{\boldsymbol{H}}_{bm}\dot{\boldsymbol{q}} + (\boldsymbol{U} - \boldsymbol{H}_{bm}^{+}\boldsymbol{H}_{bm})\boldsymbol{\zeta}, \tag{6}$$

where $\boldsymbol{U} \in \Re^{n\times n}$ stands for the unit matrix, $\boldsymbol{\zeta} \in \Re^n$ is arbitrary, and $(\boldsymbol{U} - \boldsymbol{H}_{bm}^{+}\boldsymbol{H}_{bm})$ denotes a projector onto the kernel of the inertia coupling matrix. The last term on the RHS is called the *Reaction Null Space* [1].

D. Reactionless Motion Plus Vibration Suppression Control

The two control accelerations derived above can be combined as follows:

$$\ddot{\boldsymbol{q}}_c = \boldsymbol{H}_{bm}^{+}(\boldsymbol{G}_b\boldsymbol{\nu}_b - \dot{\boldsymbol{H}}_{bm}\dot{\boldsymbol{q}}) + (\boldsymbol{U} - \boldsymbol{H}_{bm}^{+}\boldsymbol{H}_{bm})\boldsymbol{\zeta}. \tag{7}$$

With this control acceleration, both reactionless motion and vibration suppression, if vibration is present, can be achieved.

III. Models and Equation of Motion for JEMRMS and SFA

A. Models

The kinematic models with parameters for JEMRMS and SFA are shown in Figs. 2 and 3, respectively.

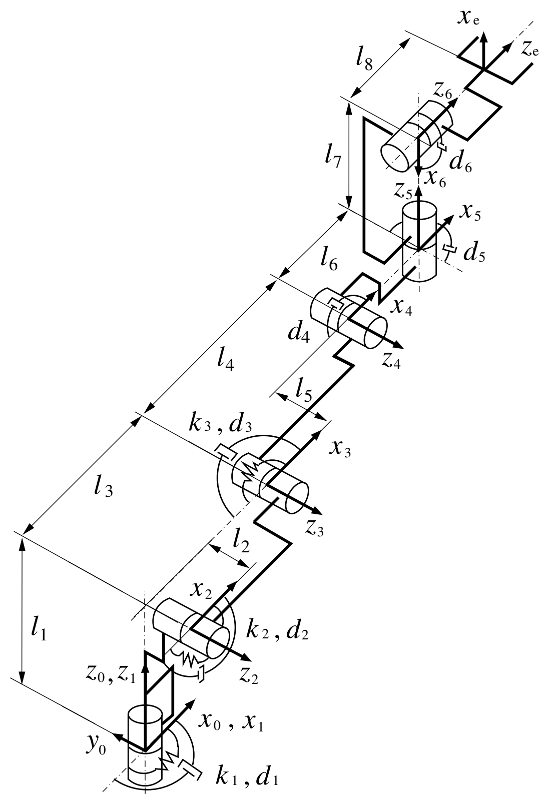

Fig. 2. Model of JEMRMS.

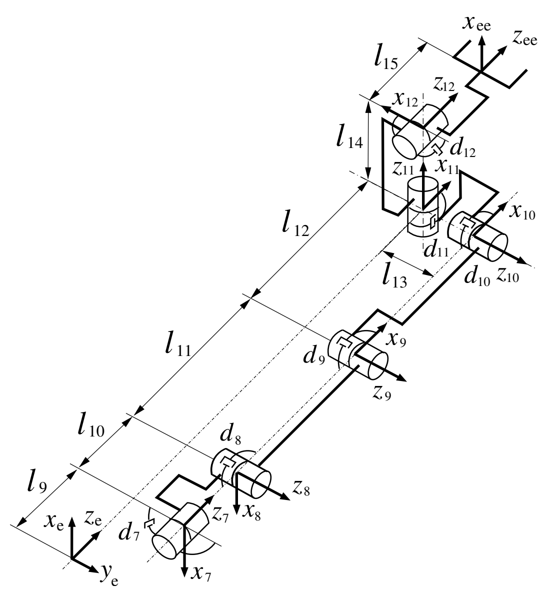

Fig. 3. Model of SFA.

Besides the kinematic parameters, the models include joint viscous damping in all joints, and joint torsional springs in the first three joints of JEMRMS. Indeed, it was pointed out [20] that the prevailing flexibilities in the large JEMRMS are in the joints, rather than in the links. The first three joints tend to deflect mostly, so we consider the subchain of the JEMRMS that includes these three joints to constitute the flexible base. The rest of the structure (including the three proximal joints of JEMRMS plus the six SFA joints) is regarded as a nine-DOF redundant mini manipulator (see Fig. 4). The values of the parameters, link lengths ($l_1 - l_{12}$), viscous damping ($d_1 - d_{12}$) and spring coefficients ($k_1 - k_3$), are given in Table I in the Appendix.

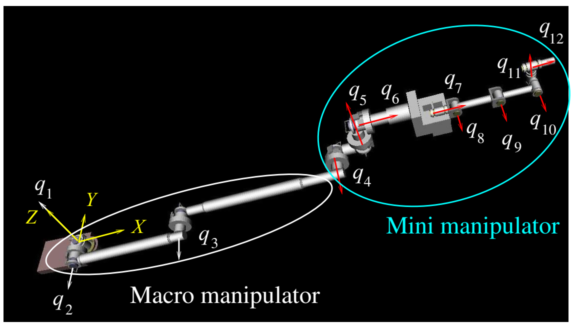

Fig. 4. JEMRMS and SFA.

It must be noted that the axes of joints #3 and #4 of the mini arm (with joint variables q_6 and q_7), are parallel, and only slightly displaced. This means that one of the DOF's of the mini arm will influence the motion very little. Nevertheless, below we will use the faithful model, without any reduction.

We note also that JEMRMS has joint angle sensors both at the motor axes (resolvers) and at the output axes (optical encoders) [20]. Hence, it is possible to evaluate the vibration in the joints constituting the flexible base, as required by the proposed control law.

B. Equation of Motion

We rewrite the equation of motion, as in (1), in the following form:

$$\begin{bmatrix} \boldsymbol{H}_M & \boldsymbol{H}_{Mm} \\ \boldsymbol{H}_{Mm}^T & \boldsymbol{H}_m \end{bmatrix} \begin{bmatrix} \ddot{\boldsymbol{q}}_M \\ \ddot{\boldsymbol{q}}_m \end{bmatrix} + \begin{bmatrix} \boldsymbol{D}_M & \boldsymbol{0} \\ \boldsymbol{0} & \boldsymbol{D}_m \end{bmatrix} \begin{bmatrix} \dot{\boldsymbol{q}}_M \\ \dot{\boldsymbol{q}}_m \end{bmatrix} + \begin{bmatrix} \boldsymbol{K}_M & \boldsymbol{0} \\ \boldsymbol{0} & \boldsymbol{0} \end{bmatrix} \begin{bmatrix} \boldsymbol{q}_M \\ \boldsymbol{q}_m \end{bmatrix} + \begin{bmatrix} \boldsymbol{c}_M \\ \boldsymbol{c}_m \end{bmatrix} = \begin{bmatrix} \boldsymbol{0} \\ \boldsymbol{\tau} \end{bmatrix}, \quad (8)$$

where $\boldsymbol{q}_m \in \Re^9$ is the joint angle vector of the mini manipulator, measured at the motor axis via the resolvers, $\boldsymbol{H}_m(\boldsymbol{q}_m) \in \Re^{9\times 9}$ is the inertia matrix of the mini manipulator and $\boldsymbol{q}_M \in \Re^3$ is the joint angle vector of the macro manipulator measured at the output axes via the optical encoders. Matrix $\boldsymbol{H}_{Mm}(\boldsymbol{q}_M, \boldsymbol{q}_m) \in \Re^{3\times 9}$ is the inertia coupling matrix, $\boldsymbol{H}_M(\boldsymbol{q}_M, \boldsymbol{q}_m) \in \Re^{3\times 3}$, $\boldsymbol{D}_M \in \Re^{3\times 3}$ and $\boldsymbol{K}_M \in \Re^{3\times 3}$ are inertia, damping and stiffness matrices of the macro manipulator. $\boldsymbol{c}_M(\boldsymbol{q}_M, \dot{\boldsymbol{q}}_M, \boldsymbol{q}_m, \dot{\boldsymbol{q}}_m) \in \Re^3$ and $\boldsymbol{c}_m(\boldsymbol{q}_M, \dot{\boldsymbol{q}}_M, \boldsymbol{q}_m, \dot{\boldsymbol{q}}_m) \in \Re^9$ denote velocity-dependent nonlinear terms, $\boldsymbol{D}_m \in \Re^{9\times 9}$ stands for mini manipulator joint damping and $\boldsymbol{\tau} \in \Re^9$ is the mini manipulator joint torque vector.

We must note that in previous works on JEMRMS/SFA, e.g. in [15], [18], the flexible base was modeled as a single flexible body with six independent flexural coordinates. This representation requires an additional mapping from the flexible joint variables of the macro arm to the flexural variables concentrated at the tip of the macro arm/base of the mini arm. In our model, we prefer to keep things simple and use the flexible joint variables per se.

IV. Control Laws

A. Resolved Accelerartion Control for End-Effector Motion

End-effector path tracking control is envisioned according to the following control law:

$$\dot{\boldsymbol{\nu}}_{ref} = \dot{\boldsymbol{\nu}}_d + \boldsymbol{K}_v(\boldsymbol{\nu}_d - \boldsymbol{\nu}) + \boldsymbol{K}_p \Delta\boldsymbol{\xi}, \quad (9)$$

where $\dot{\boldsymbol{\nu}}_d$ denotes desired spatial acceleration, $\Delta\boldsymbol{\xi}$ is the spatial displacement error, and $\boldsymbol{\nu}_d - \boldsymbol{\nu}$ is the spatial velocity error. $\boldsymbol{K}_v$ and $\boldsymbol{K}_p$ are positive-definite feedback gains.

The reference joint acceleration is written as:

$$\ddot{\boldsymbol{q}}_{ref} = \boldsymbol{J}_m^+(\dot{\boldsymbol{\nu}}_{ref} - \dot{\boldsymbol{J}}_m \dot{\boldsymbol{q}}_m), \quad (10)$$

where $\boldsymbol{J}_m$ is the mini manipulator Jacobian.

Finally, we obtain the control torque by plugging control acceleration (10) into the lower part of (8):

$$\boldsymbol{\tau}_{racc} = \boldsymbol{H}_m \boldsymbol{J}_m^+(\dot{\boldsymbol{\nu}}_{ref} - \dot{\boldsymbol{J}}_m \dot{\boldsymbol{q}}_m) - \boldsymbol{D}_{mc} \dot{\boldsymbol{q}}_m. \quad (11)$$

B. Integrated Motion Control

Reactionless motion plus vibration suppression control can be achieved with the help of the following mini arm control acceleration, derived after (7):

$$\ddot{\boldsymbol{q}}_m = \boldsymbol{H}_{Mm}^+(\boldsymbol{G}_M \dot{\boldsymbol{q}}_M - \dot{\boldsymbol{H}}_{Mm} \dot{\boldsymbol{q}}_m) + \boldsymbol{P}_{RNS}\boldsymbol{\zeta}, \quad (12)$$

where $\boldsymbol{G}_M$ is a joint damping control gain for the macro manipulator and $\boldsymbol{P}_{RNS} = \boldsymbol{U} - \boldsymbol{H}_{Mm}^+ \boldsymbol{H}_{Mm}$ is the projector onto the kernel of the inertia coupling matrix.

Further on, end-effector path tracking control will be included in the above control law by making use of the arbitrary vector ζ, in accordance with the method proposed in [1]. We have:

$$\boldsymbol{P}_{RNS}\boldsymbol{\zeta} = (\boldsymbol{J}_m(\boldsymbol{U} - \boldsymbol{H}_{Mm}^+ \boldsymbol{H}_{Mm}))^+ (\dot{\boldsymbol{\nu}}_{ref} - \dot{\boldsymbol{J}}_m \dot{\boldsymbol{q}}_m + \boldsymbol{J}_m \boldsymbol{H}_{Mm}^+ \dot{\boldsymbol{H}}_{Mm} \dot{\boldsymbol{q}}_m). \quad (13)$$

Finally, we obtain the control torque by plugging control acceleration (12) into the lower part of (8):

$$\boldsymbol{\tau}_{imc} = \boldsymbol{H}_m(\boldsymbol{H}_{Mm}^+ \boldsymbol{G}_M \dot{\boldsymbol{q}}_M - \boldsymbol{H}_{Mm}^+ \dot{\boldsymbol{H}}_{Mm} \dot{\boldsymbol{q}}_m + \boldsymbol{P}_{RNS}\boldsymbol{\zeta}) + \boldsymbol{c}_m - \boldsymbol{H}_m \boldsymbol{H}_{Mm}^+ \boldsymbol{c}_M + \boldsymbol{D}_{mc} \dot{\boldsymbol{q}}_m. \quad (14)$$

Here, $\boldsymbol{D}_{mc}$ denotes a positive definite control damping matrix for the joints of the mini manipulator. The joint damping

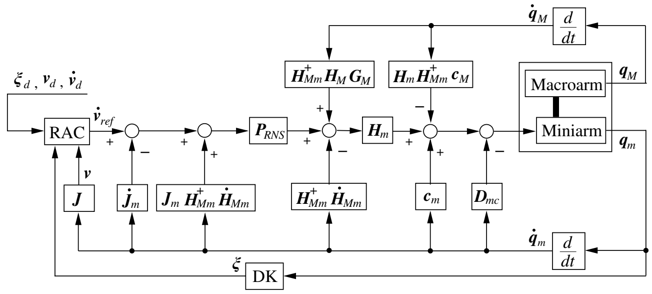

Fig. 5. Block diagram of the integrated motion controller.

term is needed to damp out coupling momentum, which is conserved after completing the vibration damping subtask.

The block scheme of the respective controller is shown in Fig. 5. The RAC block denotes the PD control for the end-effector, as in (9). DK stands for direct kinematics.

V. Simulations

Two simulations were performed:

1) Resolved acceleration control of the mini manipulator along a straight-line path with constant end-effector orientation;
2) Integrated control along the same path.

We use MaTX simulation environment [21] and the respective SpaceDynX toolbox for modeling and control of space robots.

The initial configurations for the macro and the mini manipulators was set to $\boldsymbol{q}_M = [0.0, 30.0, -30.0]^T$ deg, $\boldsymbol{q}_m = [20.0, 1.0, 1.0, 0.0, 30.0, -30.0, 20.0, -1.0, 0.0]^T$ deg, respectively. The desired position/orientation of the end-effector of the mini manipulator was set to $[-0.1, 0.1, -0.1]^T$ m, and $[-0.05, -0.05, 0.05]^T$ rad, respectively. The speed and the acceleration along the straight-line path were calculated with the help of a 5th-order spline, the final time set to 2 s. The sampling time was set to 1 ms, the total time of the simulation — to 60 s. The gain matrices were set as follows:

$$
\begin{aligned}
\boldsymbol{K}_M &= \mathrm{diag}[8000, 8000, 8000]\ \mathrm{Nm}^{-1}\\
\boldsymbol{D}_M &= \mathrm{diag}[1000, 1000, 1000]\ \mathrm{Nsm}^{-1}\\
\boldsymbol{D}_m &= \mathrm{diag}[0.1, 0.1, 0.1, 0.1, 0.1, 0.1, 0.1, 0.1, 0.1]\ \mathrm{Nsm}^{-1}\\
\boldsymbol{K}_d &= \mathrm{diag}[50, 50, 50, 10, 10, 10]\ \mathrm{s}^{-1}\\
\boldsymbol{K}_p &= \mathrm{diag}[1000, 1000, 1000, 500, 500, 500]\ \mathrm{s}^{-2}\\
\boldsymbol{D}_{mc} &= \mathrm{diag}[0.1, 0.1, 5.0, 5.0, 0.1, 0.1, 0.1, 0.1, 0.1]\ \mathrm{Nsm}^{-1}\\
\boldsymbol{G}_M &= \mathrm{diag}[2.0, 2.0, 2.0]\ \mathrm{s}^{-1}
\end{aligned}
$$

The results from the two simulations are shown in Figs. 6 and 7, respectively. In both figures, (a) and (d) denote joint angles, (b) and (e) stand for joint velocities of the macro and mini manipulators, (c) and (f) display the path of a specific point on the end-effector in the $X-Y$ and $X-Z$ planes (cf. Fig. 4), (g) and (h) are position/orientation errors of the end-effector, and (i) is the joint torque of the mini manipulator.

From Figs. 6 (a) and (b) it is seen that, under resolved acceleration control, the flexible joints of the macro arm vibrate during the whole motion. On the other hand, from Figs. 7 (a) and (b) it is apparent that the amplitude of the vibrations, in case of integrated control, is much lower (almost zero), and that vibrations damp out after approx. 20 s.

From Figs. 6 (c) and (f) it can be seen that, under resolved acceleration control, the end-effector deviates from the desired straight-line path significantly. It is seen also that after arriving at the destination, the end-effector continues to vibrate. On the other hand, from Figs. 7 (c) and (f) is becomes apparent that, under the integrated control, the end-effector tracks the desired path, and that no vibrations are observed after completing the path. The same results can be confirmed from the position error graphs in Figs. 6 (g) and 7 (g).

Finally, from Figs. 6 (i) and 7 (i) it can be concluded that the torque graphs do not exceed the torque limits of the JEMRMS/SFA system [20], and hence, the generated trajectory is feasible.

VI. Conclusions

We have shown that the integrated control method proposed previously for flexible base manipulators to ensure simultaneous end-effector path tracking, reactionless motion and vibration suppression [1], can be adapted to a real system like the JEMRMS/SFA, part of the Japanese experimental module "Kibo" on the International Space Station. It should be noted, however, that due to the highly nonlinear problem at hand, simultaneous vibration suppression and reactionless end-effector path tracking control can be realized only within rather narrow portions of the workspace. We intend to tackle the problem in a future work.

References

[1] D. N. Nenchev et. al, "Reaction Null-Space control of flexible structure mounted manipulator systems," *IEEE Tr. on Robotics and Automation*, Vol. 15, No. 6, December 1999, pp. 1011–1023.

[2] J. F. Jansen et. al, "Long-reach manipulation for waste storage tank remediation," *ASME J.*, Vol. 31, 1991, pp. 67–73.

[3] D.-S. Kwon et. al, "Input shaping filter methods for the control of structurally flexible, long-reach manipulators," *in Proc. IEEE Int. Conf. Robot. Automat.*, San Diego, CA, 1994, pp. 3259–3264.

[4] M. A. Torres and S. Dubowsky, "Path-planning in elastically constrained space manipulator systems," *in Proc. IEEE Int. Conf. Robot. Automat.*, Atlanta, GA, 1993, pp. 812–817.

[5] C. Vallancourt and C. M. Gosselin, "Compensating for the structural flexibility of the SSRMS with the SPDM," *in Proc. 2nd Workshop Robot. Space, Canadian Space Agency*, Montreal, PQ, Canada, July 1994.

[6] M. F. Stieber, C. P. Trudel, D. G. Hunter, "Robotic systems for the International Space Station," *in Proc. IEEE Int. Conf. Robot. Automat.*, Albuquerque, NM, 1997, 3068–3073.

[7] Jun Ueda and Tsuneo Yoshikawa, "Mode-Shape Compensator for Improving Robustness of Manipulator Mounted on Flexible Base," IEEE Tr. on Robotics and Automation, vol. 20, no. 2, pp. 256–268, April 2004.

[8] S. H. Lee and W. J. Book, "Robot vibration control using inertial damping forces," *in Proc. 8th CISM. IFToMM Symp. RoManSy 8*, Cracow, Poland, 1990, pp. 252–259.

[9] M. A. Torres, S. Dubowsky, and A. C. Pisoni, "Vibration control of deployment structures' long-reach manipulators: The P-PED method," *in Proc. 1996 IEEE Int. Conf. Robot. Automat.* , Minneapolis, MN, Apr. 1996, pp. 2498–2504.

[10] J. Y. Lew and D. J. Trudnowski, "Vibration control of a micro/macro manipulator system," *IEEE Contr. Syst. Mag.*, Vol. 16, No. 1, Feb. 1996, pp. 26–31.

[11] I. Sharf, "Active damping of a large flexible manipulator with a shortreach robot," *Trans. ASME, J. Dyn. Syst. Meas. Contr.*, Vol. 118, Dec. 1996, pp. 704–713.

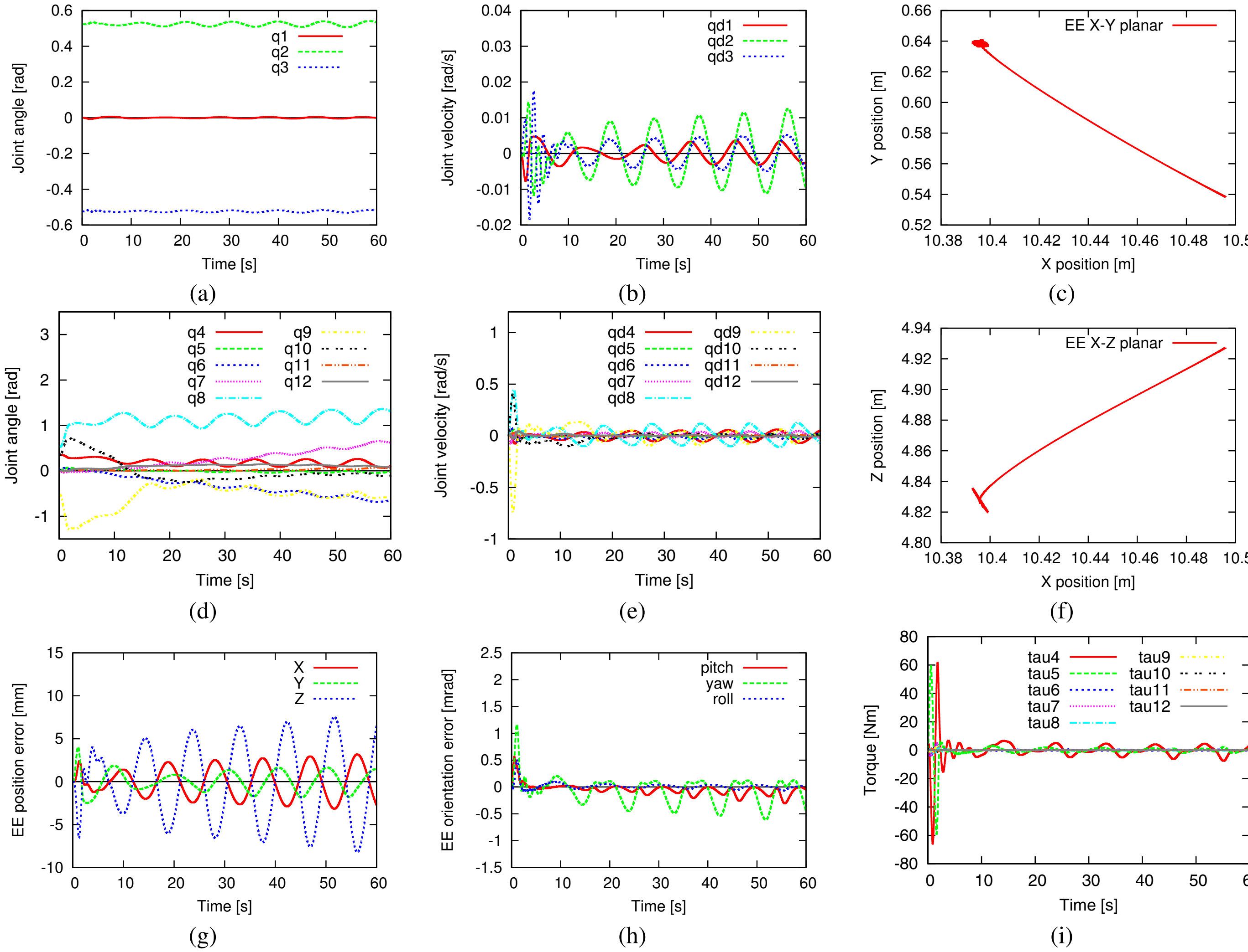

Fig. 6. Resolved acceleration control. (a) and (d) denote joint angles. (b) and (e) stand for joint velocities of the macro and mini manipulators. (c) and (f) display the path of a specific point on the end-effector in the $X-Y$ and $X-Z$ planes (cf. Fig. 4). (g) and (h) are position/orientation errors of the end-effector. and (i) is the joint torque of the mini manipulator.

[12] D. W. Cannon et al, “Experimental study on micro/macro manipulator vibration control,” *in Proc. IEEE Int. Conf. Robot. Automat.* , Minneapolis, MN, 1996, pp. 2549–2554.

[13] R. H. Cannon, Jr. and E. Schmitz, “Initial experiments on the end-point control of a flexible one-link robot,” *Int. J. Robot. Res.*, Vol. 3, No. 3, 1984, pp. 62–75.

[14] C. Mavroidis, S. Dubowsky, and V. Raju, “End-point control of long reach manipulator systems,” *in Proc. 9th World Congr. IFToMM*, Milano, Italy, 1995, pp. 1740–1744.

[15] S. Abiko and K. Yoshida, ”An Adaptive Control of a Space Manipulator for Vibration Suppression,” in *Proc. of the 2005 IEEE/RSJ International Conference on Intelligent Robots and Systems*, pp. 2888–2893, August, 2005.

[16] M. L. Hanson and R. H. Tolson, “Reducing flexible base vibrations through local redundancy resolution,” *J. Robot. Syst.*, Vol. 12, No. 11, 1995, pp. 767–779.

[17] T. Hishinuma and D. N. Nenchev, “Singularity-consistent vibration suppression control with a redundant manipulator mounted on a flexible base,” *in Proc. of the IEEE/RSJ Int. Conf. on Intelligent Robots and Systems*, Beijing, China, October, 9–15, 2006, pp. 3237–3242.

[18] K. Yoshida, H. Watanabe, S. Abiko, Y. Sato, ”Hybrid Simulation of Space Station Based Manimulator System and Vibration Suppression Control by Using the Redundancy,” Proc. of the 2005 JSME Conf. on Robotics and Mechatronics, Kobe, Japan, June 9–11, 2005. (in Japanese)

[19] S. H. Lee and W. J. Book, ”Robot vibration control using inertial damping forces,” in *Proc. 8th CISM-IFToMM Symp. RoManSy 8*, Cracow, Poland, 1990, pp. 252–259

[20] Y. Wakabayashi, H. Morimoto, N. Satoh, M. Hayashi, Y. Aiko, and M. Suzuki, ”Performance of Japanese Robotic Arms of the International Space Station,” IEEE Tr.on Robotics and Automation, vol. 15, no. 6, pp. 1011–1023, 1999.

[21] M. Koga and K. Furuta, ”MaTX: A High-Performance Programming Language (Interpreter and Compiler) for Scientific and Engineering Compuation,” IEEE Symposium on Computer-Aided Control System Design, pp. 15–22, 1992.

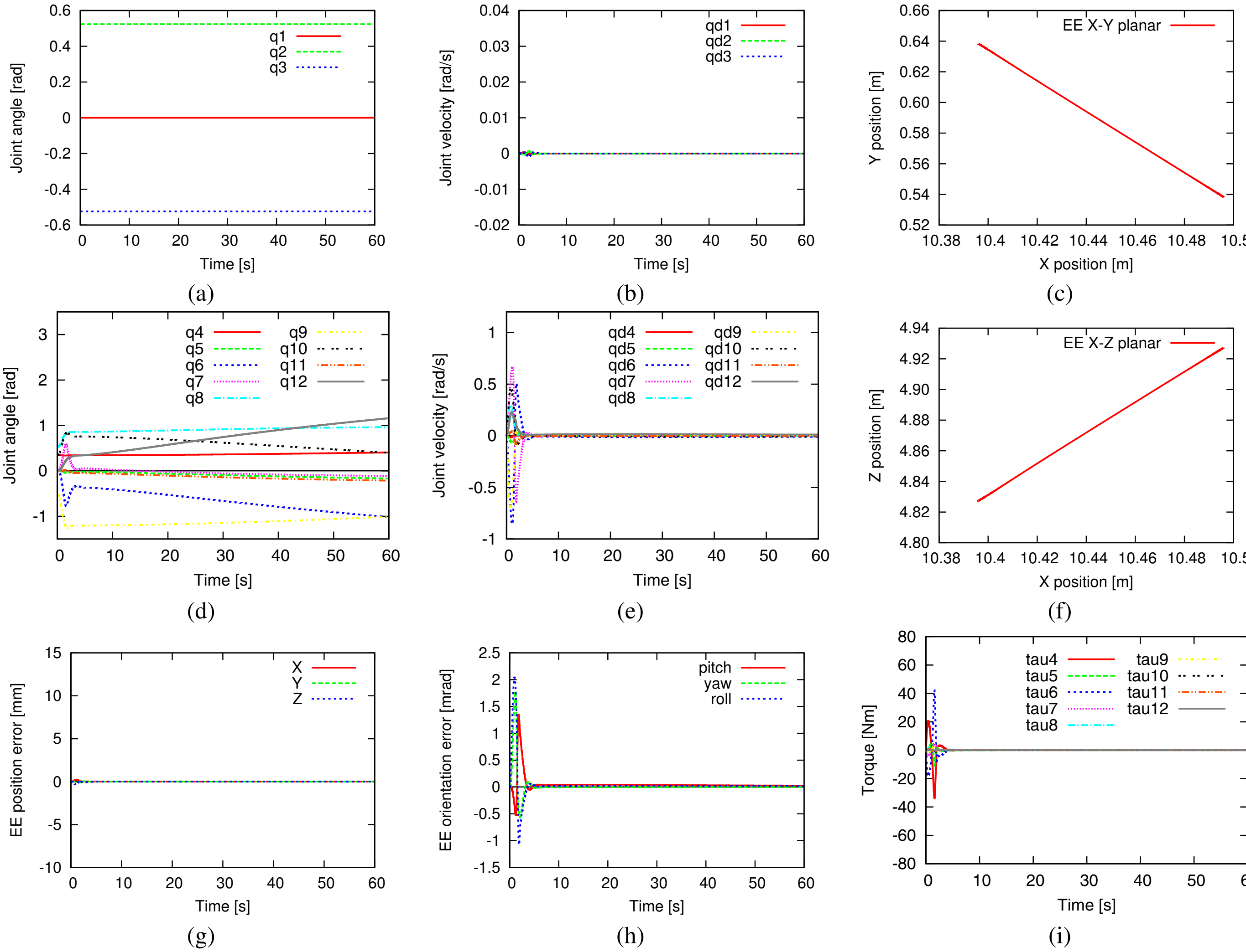

Fig. 7. Integrated control.

APPENDIX

TABLE I
PARAMETER OF JEMRMS AND SFA

Number	l [m]	k [Nm^{-1}]	d [Nsm^{-1}]
1	0.500	8000	1.0
2	0.500	8000	1.0
3	3.932	8000	1.0
4	3.945	–	0.1
5	0.500	–	0.1
6	0.440	–	0.1
7	0.500	–	0.1
8	1.590	–	0.1
9	0.3964	–	0.1
10	0.200	–	0.1
11	0.435	–	0.1
12	0.435	–	0.1
13	0.180	–	–
14	0.180	–	–
15	0.441	–	–

TABLE II
INERTIA PARAMETER OF JEMRMS/SFA AND COM
POSITION OF LINK

Link	Mass [kg]	Inertia [kgm^2]			CoM [m]		
-	m	I_{xx}	I_{yy}	I_{zz}	X	Y	Z
1	120	7.075	7.075	1.35	0.000	0.000	0.521
2	180	2.025	184.7625	184.7625	1.966	-0.500	0.521
3	180	2.025	184.7625	184.7625	5.9045	0.000	0.521
4	80	4.716	4.7167	0.90	8.097	0.500	0.521
5	80	1.5167	1.5167	0.90	8.317	0.500	0.771
6	120	4.80	4.80	2.40	9.907	0.500	1.021
7	80	0.7167	0.7167	0.90	10.4034	0.680	1.201
8	20	0.2560	0.4655	0.4655	10.7209	0.680	1.201
9	20	0.2560	0.4655	0.4655	11.1559	0.680	1.201
10	15	0.1344	0.1344	0.1687	11.3734	0.590	1.201
11	15	0.1344	0.1344	0.1687	11.3734	0.500	1.291
12	30	0.2688	0.2688	0.3375	11.5939	0.500	1.381